

# A Wide-Field H I Study of the NGC 1566 Group<sup>\*</sup>

Virginia A. Kilborn<sup>1,2</sup>, Bärbel S. Koribalski<sup>2</sup>, Duncan A. Forbes<sup>1</sup>,  
David G. Barnes<sup>3</sup>, Ruth C. Musgrave<sup>1</sup>

<sup>1</sup>Centre for Astrophysics & Supercomputing, Swinburne University of Technology, Mail 31, PO Box 218, Hawthorn, VIC 3122, Australia

<sup>2</sup>Australia Telescope National Facility, CSIRO, P.O. Box 76, Epping, NSW 1710, Australia

<sup>3</sup>School of Physics, University of Melbourne, Parkville, VIC 3010, Australia

Received date; accepted date

## ABSTRACT

We report on neutral hydrogen observations of a  $\sim 5.5^\circ \times 5.5^\circ$  field around the NGC 1566 galaxy group with the multibeam narrow-band system on the 64-m Parkes telescope. We detected thirteen H I sources in the field, including two galaxies not previously known to be members of the group, bringing the total number of confirmed galaxies in this group to 26. Each of the H I galaxies can be associated with an optically catalogued galaxy. No ‘intergalactic H I clouds’ were found to an H I mass limit of  $\sim 3.5 \times 10^8 M_\odot$ . We have estimated the expected H I content of the late-type galaxies in this group and find the total detected H I is consistent with our expectations. However, while no global H I deficiency is inferred for this group, two galaxies exhibit individual H I deficiencies. Further observations are needed to determine the gas removal mechanisms in these galaxies.

**Key words:** surveys, radio lines: galaxies, galaxies: individual (NGC 1566, NGC 1533, NGC 1549, NGC 1553), galaxies: clusters: general.

## 1 INTRODUCTION

The majority of galaxies in the Universe reside in galaxy groups (e.g. Tully 1987). However the physical processes operating in groups are poorly understood, and no detailed census of their contents is available. Studies of neutral hydrogen in groups have previously concentrated almost exclusively on Hickson Compact Groups (e.g. Shostak, Allen & Sullivan 1984; Verdes-Montenegro et al. 2001), as they require small observing regions. Studies of loose groups, which are more extended, are much fewer in number. The advent of the multibeam receiver on the Parkes telescope (Staveley-Smith et al. 1996) has made the study of loose groups feasible, and the success of the instrument has been shown with new group members being found in H I surveys of optically well studied groups. For example, ten new members were found in the Centaurus A group as part of the H I Parkes All Sky Survey, HIPASS (Banks et al. 1999) and new dwarf galaxies were found in H I surveys of the NGC 5044 and NGC 1052 groups (McKay et al. 2004). Several new galaxy groups were identified in the HIPASS Bright Galaxy Catalogue (BGC, Koribalski et al. 2004).

H I surveys of groups can reveal the effects of tidal inter-

actions in these environments (Haynes, Giovanelli & Chin-carini 1984). One of the best examples of this is the VLA survey of the M81 group by Yun et al. (1994), where the H I distribution encompasses the major galaxies in the group with many streams and tidal tails. Further tidal tails were observed when the M81 group was observed during the H I Jodrell All Sky Survey, HIJASS (Boyce et al. 2001). Blind H I surveys of groups can turn up unexpected results. For example, Barnes & Webster (2001) imaged the H I environment in five nearby galaxy groups, leading to the discovery of a ring of H I gas encircling the compact core of the loose group LGG 138. H I surveys can also uncover information about galaxy formation and evolution in groups. This was the case when a large bridge of H I was discovered with Australia Telescope Compact Array (ATCA) mapping of the NGC 6221/6215 galaxy group (Koribalski & Dickey 2004).

Cold Dark Matter theory predicts many more low-mass galaxies surrounding large galaxies than are actually observed in groups (e.g. Moore et al. 1999, Klypin et al. 1999). Searches for these low-mass satellites have been made in H I in several nearby groups such as Centaurus A and Sculptor (de Blok et al. 2002), NGC 5798, 5962, 5970, 6278, 6500 and 6574 to a limit of  $\sim 7 \times 10^6 M_\odot$  (Zwaan 2001), and NGC 1808 (Dahlem et al. 2001). More recently, Pisano et al. (2004) surveyed three groups (LGG 93, LGG 180 & LGG 478), similar in size and structure to the Local Group, for low-mass H I clouds (to an H I mass sensitivity of  $\sim 10^7 M_\odot$ ). No popula-

<sup>\*</sup> The observations were obtained with the Australia Telescope which is funded by the Commonwealth of Australia for operations as a National Facility managed by CSIRO.

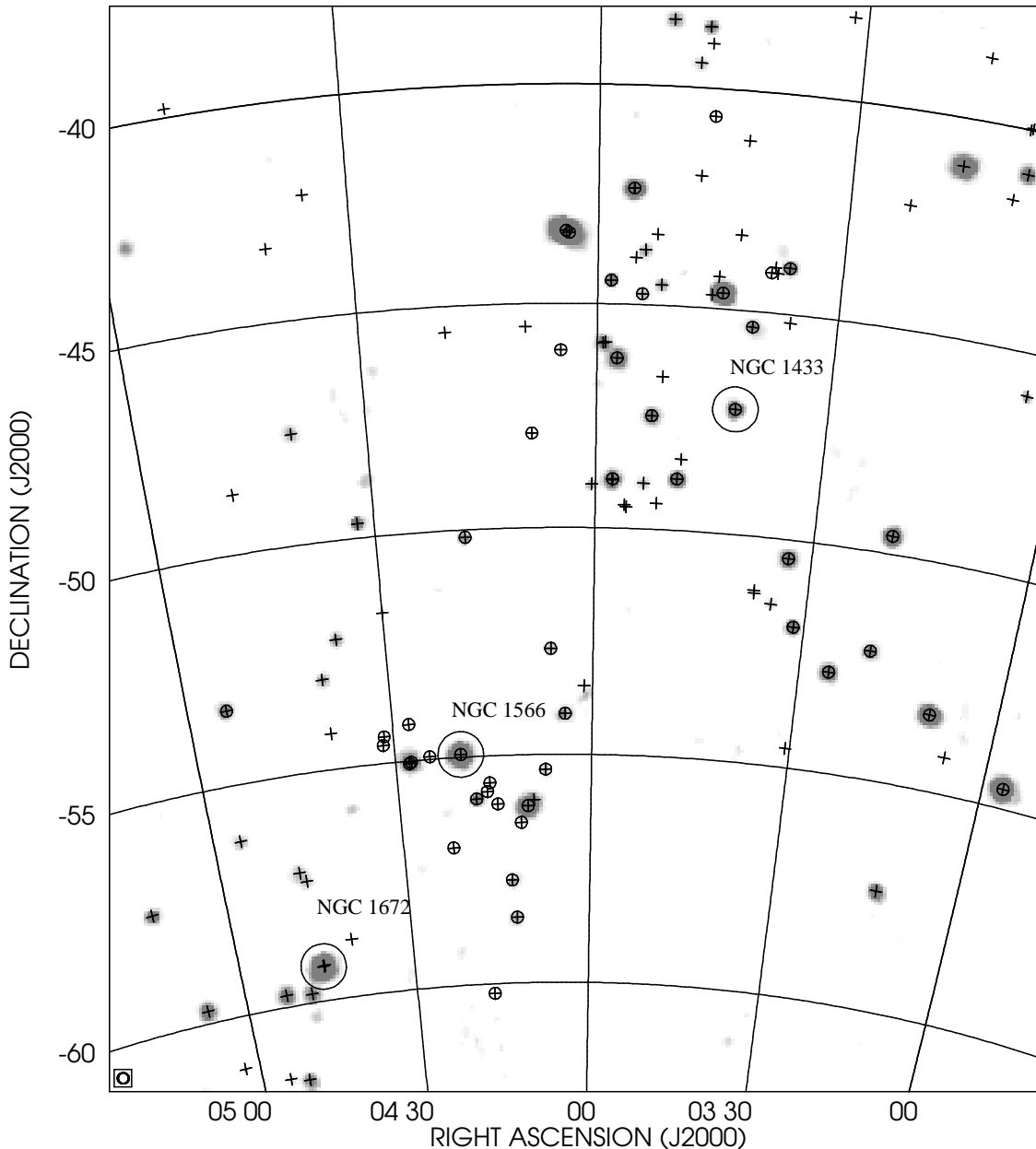


**Figure 1.** The H I-rich galaxies in the Dorado group as revealed by HIPASS. The measured H I flux densities are shown by the grey scale. The gridded beam is  $15'.5$ , and is displayed in the lower left corner. The crosses denote all galaxies in the velocity range from  $500$  to  $2400 \text{ km s}^{-1}$  recorded in NED, and the open circles denote the 46 members of the Dorado Group as listed by Maia et al. (1989). Large circles mark the galaxies NGC 1433, NGC 1566, and NGC 1672, which dominate the smaller groups within the Dorado group.

tion of H I rich satellites with little, or no optical emission were uncovered in any of the above surveys, leading to the conclusion that massive H I clouds are rare in the group environment. However, to date, no H I surveys have been deep enough to rule out a population of low-mass ( $< 10^7 M_{\odot}$ ) H I clouds.

Pointed H I surveys of groups and clusters of galaxies have generally found a trend for galaxies to be H I deficient as a function of distance from their centre. Verdes-Montenegro et al. (2001) found in a homogeneous survey of 48 Hickson Compact Groups (HCGs) that they contained only 40% of the expected H I mass, based on the optical properties of

the individual galaxies. Solanes et al. (2001) analysed the H I properties of 18 clusters, and found that two-thirds of their sample were H I deficient in the central regions (within the Abell radius). However, a recent study of the H I content of compact groups of galaxies (Stevens et al. 2004) has found no strong evidence for an H I deficiency in their sample (15 groups). Their study highlights the large uncertainties inherent in determining the expected H I mass of a galaxy based on its optical properties.

We are conducting wide-field H I observations as part of the Group Evolution Multiwavelength Study (GEMS) (Osmond & Ponman 2004, hereafter OP04; McKay et al. 2004),

containing  $\sim 60$  groups selected to have existing ROSAT PSPC X-ray observations. OP04 detail the selection criteria and X-ray properties of the groups. Seventeen of these groups in the southern hemisphere were surveyed for HI with the multibeam narrow-band system on the 64-m Parkes telescope. The main aims of this HI survey are to provide a census of the HI gas in groups, to find new group members and possible intergalactic HI clouds, and to make a direct comparison between hot and cold gas in the group environment for the first time. Here we report on our HI results for the NGC 1566 group.

### 1.1 The NGC 1566 Galaxy Group

NGC 1566 is the brightest spiral member of a nearby group of galaxies in Dorado at a distance of about 21 Mpc (OP04). This distance, and an  $H_0 = 70 \text{ km s}^{-1} \text{ Mpc}^{-1}$  is used throughout the paper. The Dorado group (see Fig. 1) consists of at least 46 galaxies (Maia et al. 1989) and covers a velocity range from  $\sim 500$  to  $2000 \text{ km s}^{-1}$ . It is part of the Fornax Wall which connects the NGC 1672, NGC 1566 and NGC 1433 galaxy groups.

Figure 1 shows the HI distribution of the Dorado group. The positions of known optical galaxies are marked. This map was derived from the HIPASS<sup>†</sup> data cubes which have a velocity resolution of  $18 \text{ km s}^{-1}$  (see Barnes et al. 2001). The AIPS task MOMNT was used with Hanning smoothing over five channels ( $65 \text{ km s}^{-1}$ , five pixels ( $20'$ ) and a flux density cutoff, after smoothing, of  $20 \text{ mJy beam}^{-1}$  per channel. The HI distribution of the region shows three distinct groupings of galaxies around the galaxies NGC 1433, NGC 1672 and NGC 1566. These three groups are at similar velocities and thus are part of the larger complex.

The NGC 1566 group has been the subject of several optical studies. Huchra & Geller (1982) catalogue 18 members in the group (which they call HG3). The group catalog by Garcia (1993) lists 6 members, and they derive a group recession velocity of  $1292 \text{ km s}^{-1}$  and a velocity dispersion of  $99 \text{ km s}^{-1}$ . Ferguson & Sandage (1990), Morshidi-Esslinger et al. (1999) and Carrasco et al. (2001) surveyed various areas of the Dorado group in the optical and cataloged large numbers of mostly low luminosity dwarf galaxies as potential members. The LEDA database lists 24 galaxies with known velocities that lie within the NGC 1566 group, while the NASA Extragalactic Database (NED) lists 22 previously catalogued galaxies in the region.

Several members of the NGC 1566 group have been previously mapped in HI at the ATCA. Walsh (2004) studied the HI dynamics of the spiral galaxy NGC 1566 itself, finding a nearly circular HI envelope, and a total dynamical mass of  $1.2 \times 10^{11} M_\odot$ . Many other observations have been made of this object, including CO (Bajaja et al. 1995), H $\alpha$  (Pence, Taylor & Atherton, 1990), HI (Reif et al. 1982), and X-ray and radio continuum (Ehle et al. 1996). NGC 1533 is a nearby, early-type galaxy with two small companions, IC 2038/9. Recent ATCA observations obtained by Ryan-Weber, Webster & Bekki (2002) reveal an asymmetric HI ring surrounding the optical galaxy, with only a small amount of HI associated with IC 2038 and none with

**Table 1.** Narrow-band observing and cube parameters.

Gridded beam size	15'5
Total observing time	18.5 hr
Velocity range	400 – 2080 $\text{km s}^{-1}$
Channel width	1.65 $\text{km s}^{-1}$
Velocity resolution	2.6 $\text{km s}^{-1}$
rms noise per channel	18.8 mJy

IC 2039. The interacting pair of galaxies NGC 1596/1602 has recently been mapped in HI at the ATCA (Chung et al. 2004).

OP04 studied the X-ray properties of the NGC 1566 group using ROSAT PSPC observations. They found galaxy halo emission around NGC 1566 itself, ( $\log L_X = 40.41 \text{ erg s}^{-1}$ , see their Table 4), but no group-scale emission. This suggests that the group is relatively young and not yet virialised. The NGC 1566 group centre and radius, as defined in the GEMS sample (see OP04, their Table 1), is  $\alpha, \delta(\text{J2000}) = 04^{\text{h}} 20^{\text{m}} 00^{\text{s}}.6, -54^{\circ} 56' 17''$  and  $r_{500} = 0.47 \text{ Mpc}$ , where  $r_{500}$  is the radius at 500 times the critical density of the Universe at the current epoch. OP04 derive a group velocity of  $v = 1402 \pm 61 \text{ km s}^{-1}$  and a velocity dispersion of  $\sigma_v = 184 \pm 47 \text{ km s}^{-1}$ , based on the nine group members within  $v \pm 3\sigma_v$  and  $r_{500}$ . The total  $B$ -band luminosity of the NGC 1566 group based on these nine members is  $1.87 \times 10^{11} L_\odot$ .

In this paper we present our HI survey of the NGC 1566 group. In Section 2 we summarize the observations and data reduction, along with the source detection and optical identification. In Section 3 we give the results from the HI survey. Discussion of the results is provided in Section 4, including the optical properties and HI content of the group, X-ray properties, and dynamics. Finally we present our conclusions in Section 5.

## 2 OBSERVATIONS AND DATA REDUCTION

Our observations of the NGC 1566 group follow the approach described in McKay et al. (2004). We scanned a field of dimensions  $5.5^\circ \times 5.5^\circ$  using the Parkes 64 m radiotelescope with the 21 cm Multibeam Receiver (Staveley-Smith et al. 1996) installed at the prime focus. Observations were acquired in the periods 2002 January 11–18, 2002 March 8–9 and 2003 May 3–5. The field was centred at  $\alpha, \delta(\text{J2000}) = 04^{\text{h}} 16^{\text{m}} 00^{\text{s}}, -55^\circ 35' 00''$ . Scans were made at a rate of one degree per minute, along lines of equatorial latitude and longitude separated by 4 arcmin. A total of 198 scans were acquired.

Data were reduced using LIVEDATA, a component of the AIPS++ package. On input, raw correlator spectra were convolved with a Hanning filter to eliminate ringing from narrow and bright emission sources. Subsequent processing steps were based on those for HIPASS data (Barnes et al. 2001) and previous GEMS data (McKay et al. 2004), with changes made to improve dynamic range near bright sources, and to track the time evolution of the (source-free) sky at higher order. Bandpass correction was applied on a per-beam, per-scan basis by iteratively clipping the data and fitting a 2nd degree polynomial to the time series of

<sup>†</sup> <http://www.atnf.csiro.au/research/multibeam>

**Table 2.** H I properties of the detected galaxies.

No.	$\alpha, \delta(\text{J2000})$ [h m s], [° ′ ″]	$v$ [km s <sup>-1</sup> ]	$w_{50}$ [km s <sup>-1</sup> ]	$w_{20}$ [km s <sup>-1</sup> ]	$S_{\text{peak}}$ [Jy]	$F_{\text{HI}}$ [Jy km s <sup>-1</sup> ]	rms [Jy]	Order	Box	$M_{\text{HI}}$ [10 <sup>8</sup> $M_{\odot}$ ]
(1)	(2)	(3)	(4)	(5)	(6)	(7)	(8)	(9)	(10)	(11)
1	4:12:11, -58:34:17	1466 ± 3	55 ± 6	102 ± 9	0.106 ± 0.009	5.7 ± 0.7	0.008	3	5	5.9 ± 0.7
2	4:10:51, -56:30:32	1310 ± 7	104 ± 14	129 ± 21	0.028 ± 0.007	2.0 ± 0.6	0.006	3	5	2.1 ± 0.6
3	4:12:39, -57:45:50	1176 ± 3	189 ± 6	214 ± 9	0.076 ± 0.008	8.7 ± 0.9	0.004	3	5	9.0 ± 0.9
4	4:27:25, -57:27:21	1215 ± 7	75 ± 14	137 ± 21	0.048 ± 0.007	3.2 ± 0.6	0.005	3	5	3.3 ± 0.6
5	4:09:42, -56:06:55	796 ± 3	247 ± 6	324 ± 9	0.382 ± 0.020	73.7 ± 2.9	0.012	3	13	76.5 ± 3.0
6	4:22:42, -56:16:59	1350 ± 4	52 ± 8	76 ± 12	0.049 ± 0.007	2.4 ± 0.5	0.005	7	5	2.5 ± 0.6
7	4:14:40, -56:04:25	1298 ± 5	189 ± 10	343 ± 15	0.140 ± 0.010	23.2 ± 1.3	0.011	3	13	24.1 ± 1.4
8	4:17:56, -55:57:06	1370 ± 2	193 ± 4	218 ± 6	0.124 ± 0.009	16.4 ± 1.1	0.004	3	5	17.1 ± 1.2
9	4:07:10, -55:18:01	1068 ± 3	99 ± 6	119 ± 9	0.073 ± 0.008	5.9 ± 0.7	0.005	3	5	6.1 ± 0.8
10	4:19:53, -54:56:46	1502 ± 1	200 ± 2	223 ± 3	1.040 ± 0.052	148.1 ± 6.4	0.009	3	13	153.9 ± 6.7
11	4:27:45, -55:01:08	1572 ± 3	93 ± 6	174 ± 9	0.283 ± 0.016	28.1 ± 1.6	0.009	3	11	29.2 ± 1.7
12	4:03:56, -54:05:04	1180 ± 2	357 ± 4	381 ± 6	0.101 ± 0.009	15.9 ± 1.1	0.004	3	5	16.5 ± 1.2
13	4:05:42, -52:41:01	902 ± 2	88 ± 4	103 ± 6	0.079 ± 0.008	4.8 ± 0.6	0.007	3	5	5.0 ± 0.7

The columns are (1) GEMS galaxy number, (2) fitted H I centre position, (3) heliocentric velocity in the optical convention, (4) 50% velocity width, (5) 20% velocity width, (6) H I peak flux density, (7) integrated H I flux density, (8) clipped rms per channel (9) Order of baseline fit to the H I spectrum, (10) Box size used to create the H I spectrum in 4′ pixels, (11) H I mass for the detection assuming cluster distance of 21 Mpc. The errors are derived following Koribalski et al. (2004).

each channel. Data acquired within 20 arcmin of known H I sources in the field (based on a first, quick process and search step) were masked during fitting to prevent contamination of the calculated bandpass. Each bandpass-removed spectrum was frame-shifted to the barycenter of the Earth-Sun system, and then baselined by subtracting a source-masked, iterative, clipped 2nd-degree polynomial fit, this time in the spectral domain.

Calibrated, processed spectra were imaged using the GRIDZILLA component of AIPS++, which is described in Barnes et al. (2001). We used the WGTMED statistic, which calculates mesh pixel values by taking the weighted median of data within 6 arcmin of the centre of each pixel.<sup>‡</sup> The weight values were directly proportional to the canonical, Gaussian observing beam profile which has a FWHM of 14.4 arcmin. We produced 2026 channel maps, centred on  $V_{\text{CMB}} = 1231.8 \text{ km s}^{-1}$ , with velocity widths of  $0.824 \text{ km s}^{-1}$ .

The gridded cube was smoothed in the spectral domain again with a Hanning filter three channels wide, and every second channel was discarded. The velocity resolution of the image was then measured, yielding a FWHM spectral resolution of  $2.6 \text{ km s}^{-1}$ . The channel separation in the final cube is  $1.65 \text{ km s}^{-1}$ . The rms noise in the final cube is measured to be  $18.8 \text{ mJy per channel}$ . The final gridded beamsize is  $15.5 \text{ arcminutes}$ , and the pixel size is  $4′ \text{ square}$ . The final cube parameters are summarised in Table 1.

## 2.1 Source Finding

The H I data cube was searched visually for sources using the KVIEW visualisation program (Gooch 1995). Two of us (VAK & RCM) catalogued sources from the original cube, and also from two smoothed versions of the cube, with final velocity resolution of  $3.3 \text{ km s}^{-1}$  and  $6.6 \text{ km s}^{-1}$ . The rms

<sup>‡</sup> For comparison, HIPASS images use the GRIDZILLA MEDIAN statistic which is the median of weighted values

in the smoothed cubes was  $11 \text{ mJy beam}^{-1}$  and  $\sim 8 \text{ mJy beam}^{-1}$  respectively. To determine the detection limit for sources in the cube, and as an extra check for the searching, twenty fake point sources were injected randomly into the original cube. These sources had a range of peak flux density between  $10\text{--}30 \text{ mJy}$ , and velocity width of  $50\text{--}500 \text{ km s}^{-1}$ . Two fake-injected cubes were made, to ensure if one of the randomly placed fake sources lay upon a real H I signal, the other cube would likely have it unobscured. Both the unsmoothed, and two smoothed versions were searched for sources, as with the original datacube. From the recovery rate of fake sources, we have determined our survey to be complete to a peak flux density limit of  $58 \text{ mJy}$  ( $\approx 3\sigma$ ) in the unsmoothed cube. While we did detect a number of sources below this limit, the sources with the lowest peak flux density were detected in the smoothed cubes only. No relationship with velocity width was seen with the detectability of these fake sources. Assuming a galaxy velocity width of  $100 \text{ km s}^{-1}$  and a Gaussian H I profile, this translates to an H I mass limit of  $3.5 \times 10^8 M_{\odot}$  ( $\sim 1 \times 10^9 M_{\odot}$  for a velocity width of  $300 \text{ km s}^{-1}$ ).

## 2.2 Derivation of the H I parameters

Once the source list was made, the H I parameters for each detection were derived using MIRIAD routines (Sault et al 1995) on the smoothed cube (velocity resolution  $6.6 \text{ km s}^{-1}$ ). A zeroth order moment map (*moment*) was made for the velocity range of emission of each detection. The central point of emission was then determined by using *imfit* to fit a 2 dimensional Gaussian to this moment map. This central position was then used in the task *mbspect* to make a spectrum of the source.

A spectrum for each source was produced using a box size of 5 pixels in width (20 arcmin), assuming a point source. The 20% and 50% velocity widths (taken as the maximum width fit in *mbspect*), integrated flux density (robust moment 0) and peak flux density for each source were also determined with *mbspect*. The heliocentric velocity for

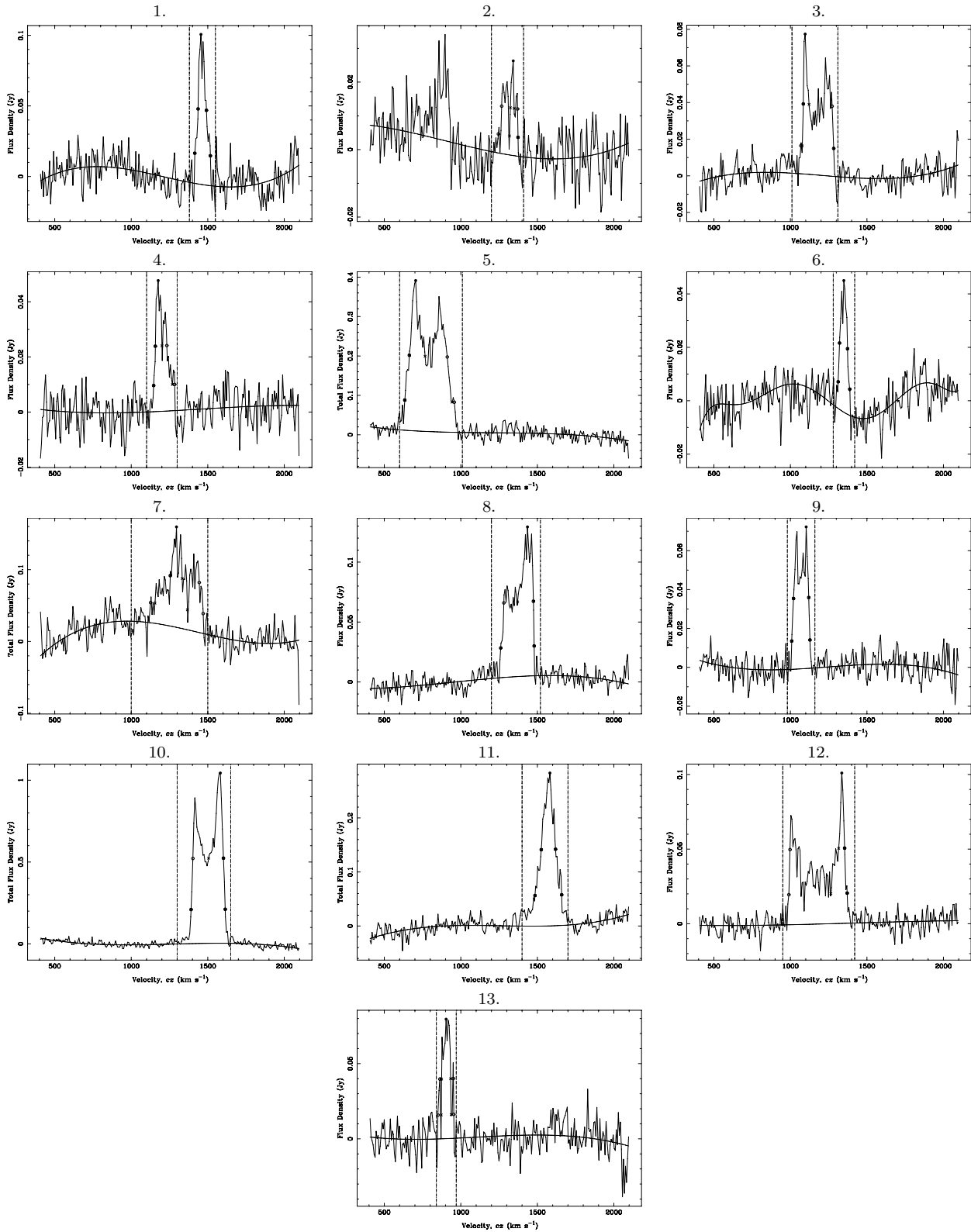


**Figure 2.** H<sub>I</sub> spectra of the thirteen galaxies detected in our NGC 1566 survey. The spectra were Hanning smoothed to a velocity resolution of  $6.6 \text{ km s}^{-1}$ . The fitted baseline is shown and the H<sub>I</sub> peak flux density is marked with a filled circle. The  $w_{20}$  and  $w_{50}$  velocity widths are shown by the open circles (outer fit), and crosses (inner fit). The velocity region between the vertical lines in the spectra was disregarded in the baseline fit.

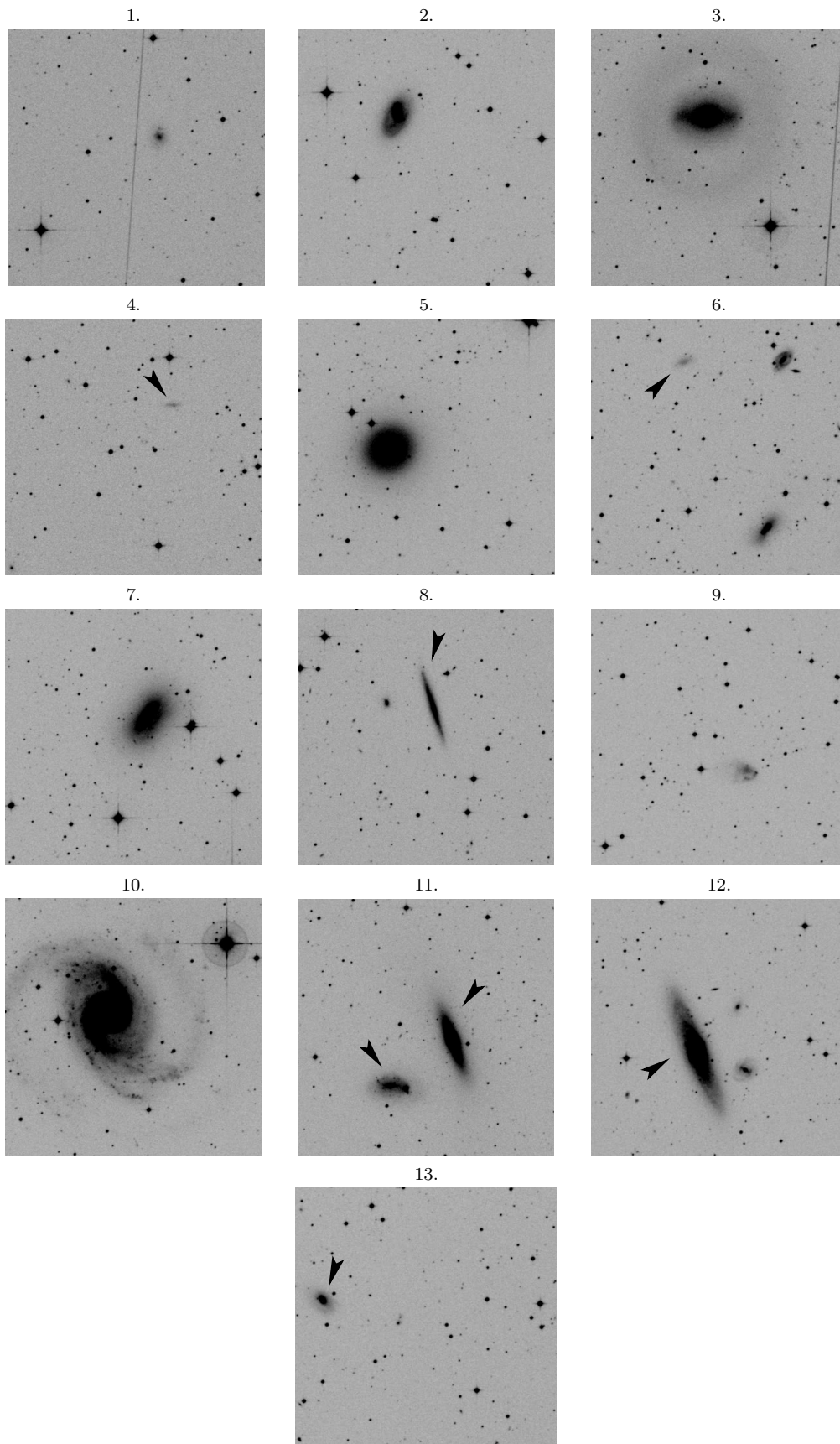


**Figure 3.** Second generation DSS *R*-band images of the thirteen galaxies detected in the NGC 1566 group. Each image is 10 arcmins across, and is centred at the HI detection. When there is more than one galaxy in the field of view, arrows indicate the matching optical counterpart, determined by either the known optical velocity of the galaxy, or in the case of #4 and #6, from high resolution ATCA observations. Note that in fields #8 and #12 there are several galaxies within the field of unknown redshift.

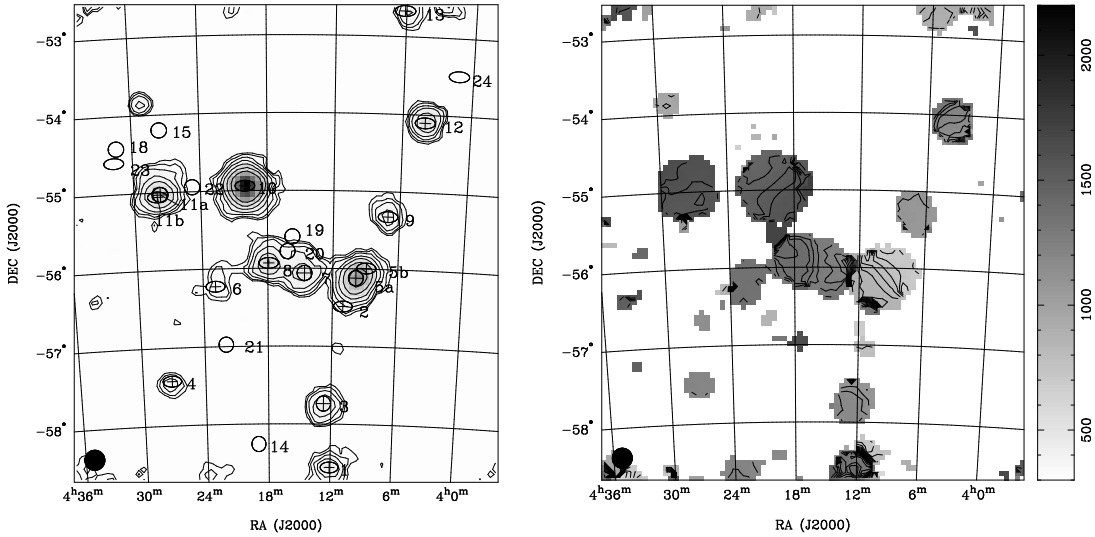


**Figure 4.** (a) The integrated H I intensity map of the NGC 1566 group as obtained from the H I Parkes narrow-band observations. The measured H I flux densities (contours) for the left image are 0.5, 1, 2, 4, 8, 16 and 32 Jy beam<sup>-1</sup> km s<sup>-1</sup>. Overplotted are the positions of known group members. The 13 crossed symbols are those detected in our H I survey, and the open symbols were undetected in H I. The circles represent E/S0 galaxies, and ellipses represent late-type galaxies. The numbers correspond with those in Table 3. Note that galaxies 16 & 17 have been previously associated with this group, but lie outside our survey region. (b) The right image shows the velocity distribution for the NGC 1566 group. The contour levels for the right image are 600 to 1615 km s<sup>-1</sup> in steps of 35 km s<sup>-1</sup>. The Parkes beam is shown in the bottom left corner of each image.

a source was determined to be the centre point of the 20% velocity width (in the optical convention).

The integrated flux density was also measured for a box size of 7 pixels to determine if any extended emission surrounded the detection. Four of the galaxies were found to have extended emission. These four sources were fitted in a similar way to above, but in this case, the flux within the box was summed rather than assuming a point source, and the box size was iteratively increased until the total flux density was constant. The final parameters for all galaxies detected in H I are given in Table 2, including the fit parameters for the spectra. The H I mass of each detection was determined using  $M_{\text{HI}} = 2.356 \times 10^5 D^2 F_{\text{HI}}$ , where  $F_{\text{HI}}$  is the integrated H I flux density in Jy km s<sup>-1</sup> (see Table 2), and  $D$  is the distance to the group in Mpc (21 Mpc for the NGC 1566 group).

H I spectra for each of the galaxies are shown in Figure 2. These spectra show the fitted baseline, the region excluded from the baseline fit with the vertical lines, and the 20% and 50% velocity widths are shown by the crosses (minimum) and circles (maximum). The peak flux density is shown with a filled circle.

Uncertainties on the derived parameters were calculated according to Koribalski et al. (2004). Detections with low H I flux have large uncertainties in the determined velocity, as do detections with asymmetric profiles. The uncertainty on the peak flux density is always greater than the rms noise of the fitted cube. Positional uncertainties are not quoted. However, the positional uncertainty of the H I detections can be calculated as the gridded beamsizes divided by the signal-to-noise (Koribalski et al. 2004).

### 2.3 Optical Identification of the H I Detections

Optical identification of the H I detections was made using the NASA Extragalactic Database (NED). A 6 arcmin region around the central point of the H I emission was searched for previously catalogued galaxies of either the same redshift or unknown redshift in NED. Table 3 gives the identifications for the H I detections, with their previously determined velocities. Eleven H I sources in the NGC 1566 group had matching optical counterparts. Of these, two H I sources (#5 and #11) correspond to catalogued galaxy pairs. The remaining two H I detections had no previously catalogued galaxy of known redshift nearby, and further high resolution observations were necessary to determine the optical counterparts to these sources (see Section 3 for details). Optical images for each detection were downloaded from the Digital Sky Survey<sup>§</sup> for each of the galaxies. These can be seen in Figure 3. The DSS images are 10 arcminutes square, and are in *R*-band. A variety of galaxy types can be seen from bright spirals and elliptical galaxies to small, faint dwarf galaxies. The optical characteristics for all galaxies are given in Table 3.

## 3 RESULTS

### 3.1 H I Properties of the NGC 1566 Group

The H I distribution for the NGC 1566 group is shown in Figure 4(a), and the mean H I velocity field is shown in Figure 4(b). These were derived from the narrow-band data

<sup>§</sup> The Digital Sky Survey, provided by the Space Science Institute, based on photographic data from the UK Schmidt Telescope.

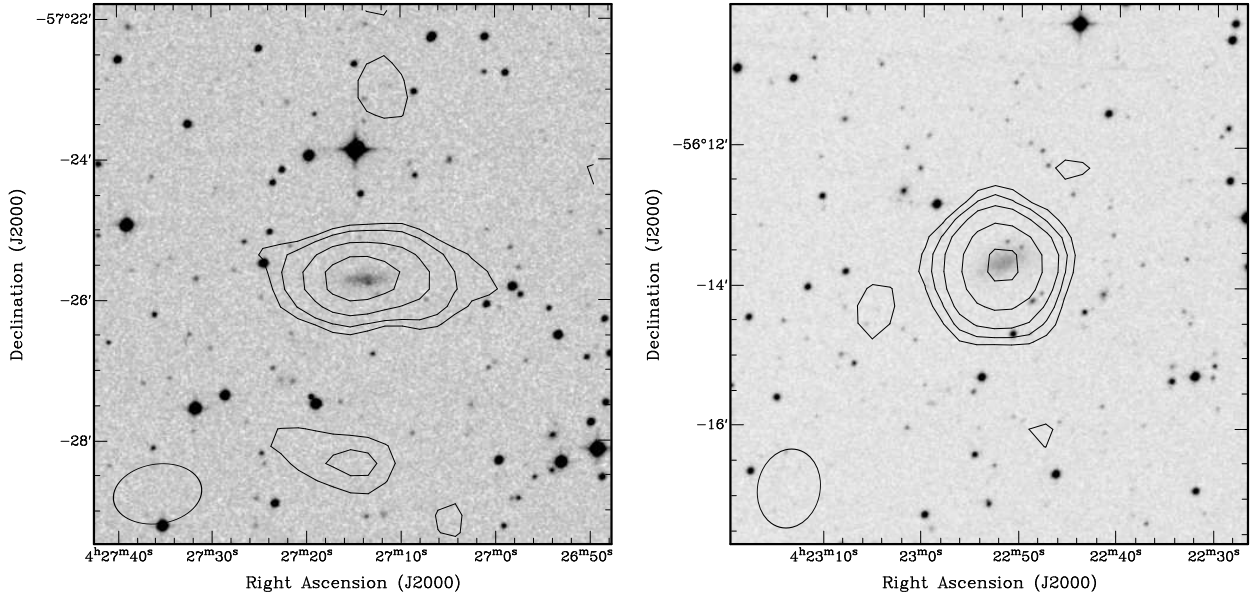


**Figure 5.** ATCA H I distribution overlaid on DSS II *R*-band images of the two new group members of the NGC 1566 group - LSBG F157-081 (left) & APMBGC 157+016+068 (right). The contour levels are 0.15, 0.25, 0.4, 0.75, 1.25  $\text{Jy km s}^{-1}$  (starting at 0.25  $\text{Jy beam}^{-1} \text{ km s}^{-1}$  for the left image). The ATCA beam is shown in the bottom left corner of each image.

cubes. After Hanning smoothing the data to the same spectral resolution as HIPASS, we used the AIPS task MOMNT (same smoothing parameters as for Figure 1) to derive these H I moment maps. Because of varying baseline curvature (see Fig. 2) these moment maps are not as sensitive as the individual H I spectra. We used a flux density cutoff of 10  $\text{mJy beam}^{-1}$ .

We detected 13 sources in the H I datacube, compared with 24 optical galaxies with known velocities in the region from LEDA. Two of the H I sources correspond to interacting galaxy pairs. We also determined the redshift for two galaxies previously not known to be group members, thus taking the number of known members for this group to 26. The spatial distribution of all known galaxies in the NGC 1566 group is over-plotted on the H I distribution in Figure 4a. The crossed symbols are those detected in H I and open symbols were not detected in our survey. The ovals represent late-type galaxies, and the circles are E/S0 galaxies. The H I distribution shows an apparent connected feature encompassing galaxies #2, #5a, #5b, #6, #7, #8 and #20. However, except for around the interacting system of NGC 1533/IC 2038, it is likely that the this apparent feature is due to smearing of the beam in the H I dataset, and higher resolution H I observations of the region are needed determine the nature of the H I distribution.

Nine known members of the NGC 1566 group were not detected in our H I survey (to an H I mass limit of  $\sim 3.5 \times 10^8 M_{\odot}$ ), and two further members were outside the survey region. We detected four E/S0 galaxies in H I but did not detect seven other early-type galaxies previously determined to be in the group. There was one irregular and one Sa galaxy not detected in H I but all other known spiral/late-type galaxies were detected in H I. NGC 1553 has previously been reported as detected in H I (de Vaucouleurs et al. 1991), however the resolution of our Parkes data is too coarse to determine a separate detection for this galaxy.

The two new group members were observed at the Australia Telescope Compact Array from 2004 March 3-7. The data were reduced using standard MIRIAD routines, and the resulting H I distributions are shown in Figure 5. Both of the H I detections correspond to previously catalogued low surface brightness irregular galaxies with blue luminosities around  $10^8 L_{\odot}$ . These two galaxies are LSBG F157-081 & APMBGC 157+016+068 (as named in NED), and both have no previous known redshift. The H I mass (as determined from the Parkes data) for the two galaxies is  $3.3 \times 10^8 M_{\odot}$  and  $2.5 \times 10^8 M_{\odot}$  respectively. Both of these new group members were unresolved in the ATCA H I maps.

The H I mass of the sources we detected in the Parkes data range from  $2.1 \times 10^8 M_{\odot}$  to  $1.4 \times 10^{10} M_{\odot}$  (see Figure 6). The highest H I mass galaxy was NGC 1566 itself. This galaxy is extended in the Parkes beam. We detect an integrated H I flux density of  $148.1 \pm 6.4 \text{ Jy km s}^{-1}$ , which is consistent with previously measured values. The HIPASS Bright Galaxy Catalogue (BGC; Koribalski et al. 2004) measured  $140 \pm 10 \text{ Jy km s}^{-1}$ , as do Mathewson & Ford (1996). Walsh (2004) measured  $147 \pm 10 \text{ Jy km s}^{-1}$  and  $161 \pm 15$  from Parkes and the ATCA respectively for NGC 1566. The total H I mass we detected in the NGC 1566 group is  $3.5 \times 10^{10} M_{\odot}$ , thus the galaxy NGC 1566 itself accounts for nearly half the H I in the group. We found that over half the galaxies in this group have H I masses less than  $10^9 M_{\odot}$ .

### 3.2 Optical Properties of the NGC 1566 group

The total *B*-band magnitudes for all known members in the NGC 1566 group are listed in Table 3. Total luminosities were determined from these magnitudes (after the magnitudes were corrected for Galactic extinction (Schlegel et al. 1998)), and are also listed in this table. The highest luminosity galaxy in the NGC 1566 group is NGC 1553, with a luminosity of  $4 \times 10^{10} L_{\odot}$ . NGC 1553 is an S0 galaxy

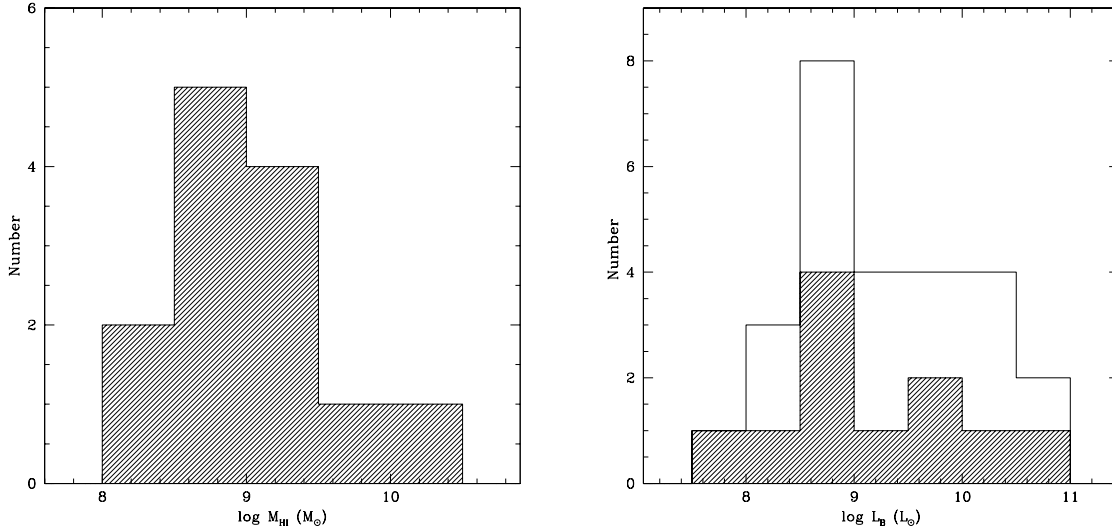


**Figure 6.** H I mass distribution for NGC 1566 group (left). Luminosity distribution for known members of the group (right). The open histogram indicates all members known optically, and the filled histogram indicates those galaxies detected in H I.

that was undetected in our H I survey. The second brightest galaxy in the group is NGC 1566 with  $L_B = 3.7 \times 10^{10} L_\odot$ . The two lowest luminosity galaxies are the two new members detected in our H I survey, LSBG F157-081 and APM-BGC 157+016+068, with luminosities of  $9 \times 10^7 L_\odot$  and  $1.3 \times 10^8 L_\odot$  respectively.

The H I mass to  $B$ -band luminosity ratio ( $M_{\text{HI}}/L_B$ ) for the galaxies in the NGC 1566 group varies from  $< 0.01$  for the early type galaxies NGC 1553 and NGC 1549, to 3.7 for the dwarf irregular galaxy LSBG F157-081. The total  $B$ -band luminosity for the group is  $1.8 \times 10^{11} L_\odot$ , compared to the total H I mass of the group of  $3.5 \times 10^{10} M_\odot$ . This gives an overall  $M_{\text{HI}}/L_B$  of  $0.19 M_\odot/L_\odot$ . The two new group members have  $M_{\text{HI}}/L_B$  of 3.7 and 1.9, which confirms H I surveys are a good way of detecting gas-rich, low luminosity group members.

Using the  $B$ -band magnitudes, we have constructed a luminosity histogram for this group. This is shown in Figure 6. Shown is the total luminosity distribution for the group, and that for only those galaxies detected in H I (NB: only single H I detections are included in the second sample). We find that the H I detected galaxies span the full range of the optical luminosity distribution, and have a similar shape to the total luminosity distribution. Similar to the H I mass distribution for this group, half of the galaxies in the group have  $L_B < 10^9 L_\odot$ . The optical galaxy numbers drop off towards  $L_B$  of  $10^8 L_\odot$ , which corresponds to the optical limit for previous redshift surveys of the region.

## 4 DISCUSSION

### 4.1 H I Content and Deficiency

H I observations of galaxies in groups and clusters have shown some galaxies to be H I deficient near the centre of the group or cluster (Solanes et al. 2001; Verdes-Montenegro et al. 2001; Giovanelli & Haynes 1985). In order to determine whether the H I content of a galaxy in a group or cluster is

deficient, normal or over-abundant, a good estimate of the expected H I is needed. The expected H I mass of isolated galaxies has been studied in the past using either the optical morphology and optical diameter of the galaxies (Solanes et al. 1996; Chamaraux et al. 1986; Haynes & Giovanelli 1984 [hereafter HG84]) or using blue magnitude and optical morphology (HG84). HG84 show that the H I content is more closely tied to the galaxy’s optical extent and morphological type, thus we use this method in the following analysis.

Optical properties for most previously catalogued galaxies in the HIPASS BGC (Koribalski et al. 2004) were obtained from LEDA, including morphological type, optical diameters and magnitudes (Koribalski et al. 2004). Following Solanes et al. (1996), we made a linear regression fit for optical diameter and H I mass to nearly 800 BGC galaxies. The galaxies were divided into morphological type from Sb to Irr, and the resulting linear regression coefficients,  $\alpha$  and  $\beta$  (such that  $M_{\text{HI},ex} = \alpha + \beta \log d$ , where  $d$  is the optical diameter of the galaxy in kpc) for each morphological type are listed in Table 4. The scatter in the H I masses,  $\sigma$ , and the number galaxies at each morphological type,  $N$ , are also given in Table 4. We use the morphology and optical diameter of the NGC 1566 group galaxies, and the coefficients given in Table 4, to determine their expected H I mass,  $M_{\text{HI},ex}$ . There are very small numbers of early-type galaxies in the BGC, thus there is a large error on calculating the expected H I mass for galaxies of optical morphology earlier than Sb. In particular, it is known that elliptical galaxies are rarely detected in H I (Sadler et al. 2001), and we do not discuss these galaxies further in this section.

We believe that the H I estimates from the BGC for late-type galaxies, especially Sd-Irr are more accurate than previous estimates. Low surface brightness late-type galaxies can be easily missed in optical surveys, and thus these potentially H I-rich galaxies will not have been included in a targeted H I survey. As late-type galaxies have a high detection rate in H I, we expect to have a more complete sample than optically based pointed H I surveys. Indeed, the lat-

**Table 3.** Group members of the NGC 1566 group. Galaxies 1-13 were detected in the H I survey, and galaxies 14-24 have optical detections only.

Galaxy No. (1)	Galaxy Name (2)	Velocity (3)	Morphology (4)	<i>B</i> -band magnitude (5)	$L_B$ (6)	$M_{\text{HI}}/L_B$ (7)
1	IC 2049 <sup>1</sup>	1086±46	Sd	14.56	6.6	0.9
2	NGC 1536	1565±104	Sc pec	13.29	21.3	0.1
3	NGC 1543	1094±32	S0	10.67	237.9	0.04
4	LSBG F157–081	...	Irr	16.72	0.9	3.7
5a	NGC 1533	668±41	S0	11.74	88.8	...
5b	IC 2038	712±52	Sd pec	14.82	5.2	...
6	APMBGC 157+016+068	...	Irr	16.32	1.3	1.9
7	NGC 1546	1160±66	S0	12.31	52.5	0.5
8	IC 2058	1268±88	Sc	13.90	12.1	1.4
9	IC 2032	1070±34	Im	14.78	5.4	1.1
10	NGC 1566	1449±19	Sbc	10.19	370.2	0.4
11a	NGC 1596	1465±24	S0	12.01	69.2	...
11b	NGC 1602	1731±31	Im	13.79	13.4	...
12	NGC 1515	1216±48	Sbc	11.96	68.5	0.2
13	NGC 1522	1012±91	pec	14.08	10.3	0.5
14	ESO 118-019 <sup>2</sup>	1133±77	S0 pec	14.90	4.8	< 0.7
15	ESO 157-030	1341±51	E4	14.30	8.4	< 0.5
16	ESO 157-047 <sup>3,4</sup>	1733±39	S0/a pec	15.52	2.7	< 1.29
17	ESO 157-049 <sup>3</sup>	1729±34	Sbc	14.37	7.9	< 0.4
18	IC 2085	1010±30	S0 pec	14.26	8.7	< 0.4
19	NGC 1549	1214±21	E0-1	10.48	283.4	< 0.01
20	NGC 1553 <sup>5</sup>	1239±18	S0	10.10	402.2	< 0.01
21	NGC 1574	925±66	S0	11.17	150.1	< 0.02
22	NGC 1581	1527±88	S0	13.36	20.0	< 0.18
23	NGC 1617	1063±21	Sa	11.35	127.2	< 0.03
24	PGC 429411	1135±40	Irr	16.19	1.5	< 2.3

The columns are: (1) GEMS galaxy number, (2) galaxy name, (3) optical velocity ( $\text{km s}^{-1}$ ) from the RC3 catalogue (de Vaucouleurs et al. 1991), except where listed in the table notes below, (4) morphological classification, (5) *B*-band magnitude, (6) *B*-band luminosity in units of  $10^8 L_\odot$ , (7)  $M_{\text{HI}}/L_B$  in units of  $M_\odot/L_\odot$ , where no value is given for the interacting galaxies, and the upper limits are based on the H I mass limit of the survey of  $3.5 \times 10^8 M_\odot$ . The *B*-band magnitudes come from the ESO-LV catalogue (Lauberts & Valentijn 1989), apart from #4 and #6, which come from Maddox et al. (1990), and #24 which is the extinction corrected total magnitude from the LEDA database.

Notes: 1. The H I velocity for this galaxy is  $1466 \pm 3 \text{ km s}^{-1}$ , which is inconsistent with the published optical value, 2. #14 Velocity from Saunders et al. (2000), 3. These galaxies have previously been associated with the NGC 1566 group but lie outside our H I survey region, 4. #16 Velocity from Loveday et al. (1996), 5. #24 Velocity from Katgert et al. (1998).

**Table 4.** Linear regression coefficients as derived from the HIPASS BGC (Koribalski et al. 2004).

Type	$\alpha$	$\beta$	$\sigma$	N
Sb	8.39	1.02	0.24	85
Sbc	8.39	1.05	0.29	130
Sc	8.30	0.99	0.27	134
Scd	7.80	1.38	0.24	88
Sd	7.12	1.97	0.26	75
Sm	7.70	1.45	0.28	84
Irr	7.29	1.9	0.33	141

est H I estimate for late-type galaxies in the literature was HG84 who have a sample size of just 7 for irregular galaxies, whereas there are 141 in the BGC. We must bear in mind that we have no indication of how many late-type galaxies were not detected in the survey, thus the upper limit to the H I mass of undetected galaxies is not included in the linear regression fit.

We have calculated the expected H I mass for each

galaxy in the NGC 1566 group, including previously catalogued members of known redshift that were not detected in our H I survey. To reduce the uncertainty in the calculation of expected H I mass, we limit our comparison to non-interacting galaxies of type Sb or later. Nine galaxies meet this criteria, including eight galaxies detected in our H I survey, and the undetected irregular galaxy PGC 429411. For comparison we calculate the expected H I mass using both the coefficients in Table 4, and those given in HG84. Figure 7 shows the expected H I mass versus the detected H I mass for the eight galaxies detected in our survey. The vertical error bars represent the scatter in the expected H I mass of a given H I mass and optical diameter for the BGC and HG84 samples. This figure shows that the expected H I mass from HG84 is always lower than that from the BGC.

The expected H I mass for most of the galaxies is consistent with what was observed, and considering the group as a whole, the NGC 1566 group does not appear to be H I deficient. Two galaxies have a slightly higher detected H I mass than was expected, and a further two galaxies display a marked H I deficiency. These latter galaxies are the Sbc

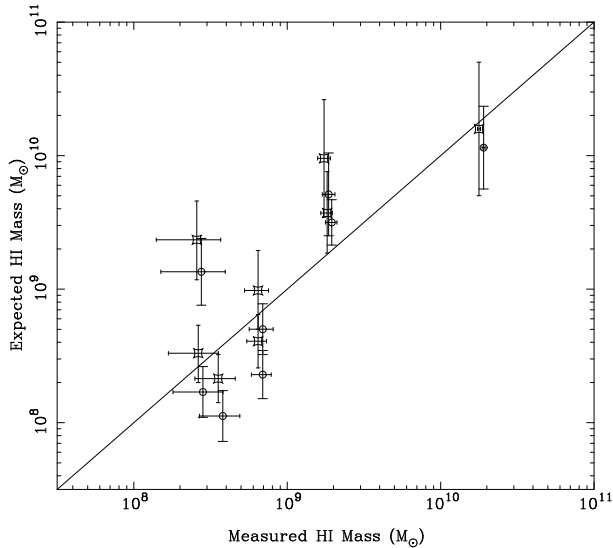


**Figure 7.** Expected H I mass of non-interacting late-type galaxies compared to the detected H I mass. The squares show the expected H I mass using the coefficients in Table 4, and the circles are the expected H I mass from the coefficients in HG84. The errors show the scatter in H I mass for a galaxy of given optical diameter and morphology.

spiral NGC 1515 and the peculiar Sc spiral NGC 1536, with 5 – 10 times less H I detected than expected. While NGC 1515 is relatively isolated, NGC 1536 is situated spatially near the interacting galaxy pair of NGC 1533/IC 2038. However there is a large velocity difference between the pair and NGC 1536 of nearly  $500 \text{ km s}^{-1}$ . The expected H I mass for the undetected irregular galaxy PGC 429411 is  $3.1 \pm 1 \times 10^8 M_{\odot}$ . As this H I mass lies near our detection limit for the H I survey, we are unable to tell whether this galaxy is H I deficient, or contains H I within the normal range.

## 4.2 Group Distribution and Dynamics

To study the dynamical state of the NGC 1566 group, we now derive the virial radius and velocity dispersion of the group members. The virial radius can be calculated using X-ray emission where the latter exists in the intra-group medium. The ROSAT PSPC data for the NGC 1566 group, along with other GEMS groups, are presented in OP04. The X-ray data cover a circular region of  $\sim 2$  degrees in diameter. OP04 find X-ray emission that is consistent with coming from NGC 1566 itself, i.e. no evidence for extended emission from the intra-group environment.

OP04 derived an  $r_{500}$  radius of 470 kpc based on the X-ray temperature of  $0.70 \pm 0.11 \text{ keV}$ . However, the X-ray emission in the NGC 1566 group is dominated by hot gas in the halo of NGC 1566 itself, which reaches the background level at a radius of 29 kpc. So the temperature-based  $r_{500}$  should be treated with some caution.

An alternative method for calculating  $r_{500}$  is to use the group’s velocity dispersion and the virial theorem (see OP04). The accuracy of this method improves with the number of reliable galaxy velocities. Based on only 9 galaxies, OP04 derive a velocity dispersion for the group of  $184 \pm 47 \text{ km/s}$ . This would translate into an  $r_{500}$  radius of 250 kpc.

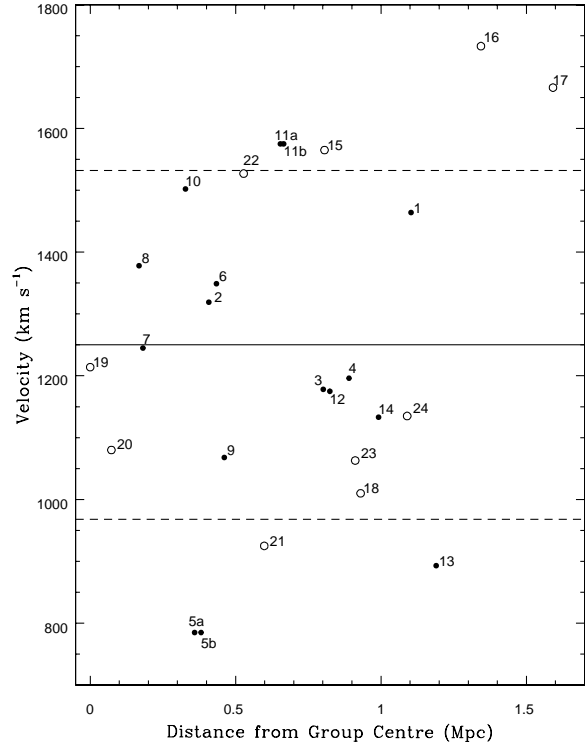


**Figure 8.** Velocity of the NGC 1566 group members versus their distance from group center. The filled circles show galaxies detected in H I and the open symbols are known galaxies in the group that we did not detect. The solid line shows the mean velocity for the group, and the dashed lines show the velocity dispersion. The virial radius for this group is 580 kpc. Galaxy #19 (NGC 1549) is taken as the centre of the group.

A better estimate of the dispersion for the group uses all known group members. Velocities were taken from the literature for the optically known galaxies not detected in our H I survey. Without removing any spatial or velocity outliers, we use a biweight estimator with bootstrap errors as per Beers et al. (1990). This gives the average velocity of the group as  $v = 1250 \pm 57 \text{ km s}^{-1}$ , and velocity dispersion of  $\sigma_v = 282 \pm 30 \text{ km s}^{-1}$ . This velocity dispersion gives a  $r_{500}$  radius of 386 kpc, and thus a virial radius,  $r_v$ , of  $\sim 580 \text{ kpc}$  for the NGC 1566 group ( $r_v \sim 3/2 \times r_{500}$ ).

Figure 8 shows the velocity distribution versus the distance from the centre of the group. The solid line and dashed lines show  $v$  and  $\sigma_v$  respectively. For this plot, the galaxy #19, NGC 1549, was chosen to be the center position as it is the brightest elliptical in the NGC 1566 group, and has a velocity very close to the mean velocity of the group.

Eleven galaxies associated with the NGC 1566 group lie within the virial radius of 580 kpc. A further 12 galaxies are located between 1 – 2  $r_v$ . As such a large number of galaxies lie beyond the virial radius, it is possible this group is young and not yet virialised. There has been recent work on the evolution of galaxies lying outside the virial radius of groups and clusters. Simulations have shown that up to half of the galaxies that lie beyond the virial radius of a cluster may have traveled through the cluster center (Gill,

Knebe & Gibson 2004; Ghigna et al. 1998). Thus the evolutionary history of these ‘backsplash’ galaxies may have been influenced by this encounter, and mass loss of up to 40% or greater might be expected. Observationally, there is some evidence of H I stripped galaxies not only in the centres of clusters (e.g. Solanes et al. 2001), but also nearer the edges of clusters (Kenney, van Gorkom & Vollmer 2004; Vogt et al. 2004; Vollmer 2003). By determining the H I content of the galaxies in the GEMS groups we will be able to see if this trend continues in the less dense group environment. We have found two H I deficient galaxies in the NGC 1566 group, NGC 1536 and NGC 1515, which lie near or beyond the virial radius of the group. High resolution H I observations of these two H I deficient galaxies combined with H $\alpha$  measurements (e.g. Vogt et al. 2004) will provide further information to the past history of these galaxies, particularly whether their gas removal mechanism is due to tidal interactions, ram pressure stripping, or a combination of the two.

## 5 CONCLUSIONS

We have conducted a blind H I survey of a region of  $5.5^\circ \times 5.5^\circ$  in the NGC 1566 group. Thirteen galaxies were detected in the H I datacube, including two LSB dwarf galaxies that had no previously known redshifts (LSBG F157-081 & APMBGC 157+016+068), which are new group members. There are now 26 known members in the NGC 1566 group. Two H I detections have two or more optical counterparts, and are previously known interacting systems that are confused within our beamsize of 15.5 arcmin (NGC 1533/IC 2038, and NGC 1602/NGC 1596). No isolated H I clouds were detected in our survey to a limit of  $\sim 3.5 \times 10^8 M_\odot$ .

The total H I mass detected in the group was  $3.5 \times 10^{10} M_\odot$ , and the galaxy NGC 1566 itself contains nearly half of the H I mass of this group, with  $M_{\text{HI}} = 1.4 \times 10^{10} M_\odot$ .

We calculate the virial radius of this group to be 580 kpc, and find over half the galaxies we associate with the group to lie beyond this radius. Thus it is possible that this is a young, non-virialised group. The total H I contained in the late-type galaxies of this group appears to be consistent with the expected H I content based on their optical diameter and morphology. However there are two cases in which a spiral galaxy appears to be 5-10 times more deficient than expected - these are NGC 1536 and NGC 1515. Further observations are needed of these two galaxies to determine their gas removal mechanisms.

## ACKNOWLEDGMENTS

Thanks to C. Mundell, N. McKay and S. Brough for help with the Parkes observations, and to R. Allen for assistance with the ATCA observations. We are grateful to D. J. Pisano and R. Braun for useful discussions relating to the data reduction, in particular ideas for source masking during bandpass estimation to improve dynamic range near bright sources. J. Osmond and T. Ponman are acknowledged for helpful discussions. We acknowledge the Parkes telescope staff and thank them for their assistance in the observations. Many thanks to M. Calabretta for continuing support

of livedata. Thankyou to the anonymous referee for helpful comments.

This research has made extensive use of the NASA/IPAC Extragalactic Database (NED) which is operated by the Jet Propulsion Laboratory, Caltech, under contract with the National Aeronautics and Space Administration. The Digitized Sky Survey was produced by the Space Telescope Science Institute (STScI) and is based on photographic data from the UK Schmidt Telescope, the Royal Observatory Edinburgh, the UK Science and Engineering Research Council, and the Anglo-Australian Observatory. VAK acknowledges the support of an ARC/CSIRO Linkage Postdoctoral Fellowship.

## REFERENCES

- Bajaja, E., Wielebinski, R., Reuter, H.-P., Harnett, J. I., Hummel, E. 1995, *A&AS*, 114, 147
- Banks, G. D., Disney, M. J., Knezek, P. M. et al. 1999, *ApJ*, 524, 612
- Barnes, D. G., Staveley-Smith, L., de Blok, W. J. G. et al. 2001, *MNRAS*, 322, 486
- Barnes, D. G., Webster, R. L. 2001, *MNRAS*, 324, 859
- Beers, T. C., Flynn, K., Gebhardt, K., 1990, *AJ*, 100, 32
- de Blok, W. J. G., Zwaan, M. A., Dijkstra, M., Briggs, F. H., Freeman, K. C. 2002, *A&A* 382, 43
- Boyce, P.J., Minchin, R. F., Kilborn, V. A. et al. 2001, *ApJL*, 560, 127
- Carrasco E.R., Mendes de Oliveira C., Infante L., Bolte M. 2001, *AJ* 121, 148
- Chamaraux, P., Balkowski, C., Fontanelli, P. 1986, *A&A*, 1986, 165
- Chung A. et al. 2004, in preparation
- Dahlem, M., Ehle, M., Ryder, S. D. 2001, *A&A* 373, 485
- Ehle, M., Beck, R., Haynes, R. F. et al. 1996, *A&A*, 306, 73
- Ferguson H.C., Sandage A. 1989, *AJ* 100, 1
- Garcia A.M. 1993, *A&AS* 100, 47
- Gooch, R. 1995, in ASP Conf. Se. 77, *Astronomical Data Analysis Software and Systems IV*, ed R. A. Shaw, H. E. Payne, J. E. Haynes (San Francisco: ASP), 144
- Ghigna, S., Moore, B., Governato, F. et al. 1998, *MNRAS*, 300, 146
- Gill, S. P. D., Knebe, A., Gibson, B. K. 2004, *MNRAS*, submitted
- Giovanelli, R. & Haynes, M. P. 1985, *ApJ*, 292, 404
- Haynes M. P. & Giovanelli, R. 1984, *AJ*, 89, 758
- Haynes, M. P., Giovanelli, R., Chincarini, G. L. 1984, *ARAA*, 22, 445
- Huchra, J. P., Geller, M. J. 1982, *ApJ*, 257, 423
- Katgert, P., Mazure, A., den Hartog, R., et al. 1998, *A&A Suppl. Ser.* 129, 399
- Kenney, J. D. P., van Gorkom, J. H., Vollmer, B. 2004, *AJ*, 127, 3375
- Klypin, A., Kravstov, A., Valenzuela, O., Prada, F. 1999, *ApJ*, 522, 82
- Koribalski, B. et al. in preparation
- Koribalski, B. & Dickey, J. M. 2004, *MNRAS*, 348, 1255
- Koribalski B. et al. 2004, *AJ*, 128, 16
- Lauberts, A. & Valentijn, E. A. 1989, in ‘‘The Surface Photometry Catalogue of the ESO-Uppsala Galaxies’’, Garching Bei Munchen: European Southern Observatory
- Loveday, J., Peterson, B. A., Maddox, S. J., Efstathiou, G. 1996, *ApJS*, 107, 201
- Maddox, S. J., Sutherland, W. J., Efstathiou, G., Loveday, J. 1990, *MNRAS*, 243, 692
- Maia M.A.G., Da Costa L.N., Latham D.W 1989, *ApJS* 69, 809
- Mathewson D.S., Ford V.L. 1996, *ApJS* 107, 97

- McKay, N. F., Mundell, C. G., Brough, S. et al. 2004, MNRAS, in press
- Moore, B., Ghigna, S., Governato, F. et al. 1999, ApJ, 524, 19
- Morshidi-Esslinger Z., Davies J.I., Smith R.M. 1999, MNRAS 304, 297
- Osmond, J.P.F., Ponman T.J. 2004, MNRAS, 350, 1511
- Pence, W. D., Taylor, K., Atherton, P. 1990, ApJ, 357, 415
- Pisano, D. J., Barnes, D. G., Gibson, B. K. et al. 2004, ApJL, 610, 17
- Reif K., Mebold, U., Goss, W.M., van Woerden, H., Siegman, B. 1982, A&A 50, 451
- Ryan-Weber, E., Webster, R., Bekki, K. 2003, in “The IGM/Galaxy Connection: The Distribution of Baryons at Z=0”, ASSL Conference Proceedings, Vol. 281, Edited by J. L. Rosenberg and M. E. Putman
- Sadler, E. M., 2001, in “Gas and Galaxy evolution”, ASP Conf. Se., 240, eds J. E. Hibbard, M. P. Rupen & J. H. van Gorkom, 445
- Sault, R. J., Teuben, P. J., Wright, M. C. H. 1995, in ASP Conf. Se. 77, Astronomical Data Analysis Software and Systems IV, ed R. A. Shaw, H. E. Payne, & J. E. Haynes (San Francisco: ASP), 433
- Saunders, W., Sutherland, W. J., Maddox, S. J. 2000, MNRAS, 317, 55
- Schlegel D.J., Finkbeiner D.P., Davis M. 1998, ApJ 500, 525
- Shostak, G. S., Allen, R. J., Sullivan, W. T III 1984, A&A, 139, 15
- Solanes, J. M, Manrique, A., Garcia-Gomez, C., et al. 2001, ApJ, 548, 97
- Solanes, J. M, Giovanelli, R., Haynes, M. P. 1996, ApJ 461, 609
- Staveley-Smith, L. et al. 1996, PASA, 13, 243
- Stevens, J. B., Webster, R. L, Barnes, D. G., Pisano, D. J., Drinkwater, M. J. 2004, PASA, in press
- Tully, R. B. 1987, ApJ, 321, 280
- de Vaucouleurs G., de Vaucouleurs A., Corwin Jr. H.G., Buta R.J., Paturel G., Fouqué P. 1991, “Third Reference Catalogue of Bright Galaxies” (New York: Springer Verlag), [RC3]
- Verdes-Montenegro, L., Yun, M. S., Williams, B. A., Huchtmeier, W. K., Del Olmo, A., Perea, J. 2001, A&A, 377, 812
- Vogt, N. P., Haynes, M. P., Giovanelli, R., Herter, T. 2004, AJ, 127, 3300
- Vollmer, B. 2003, A&A, 398, 525
- Walsh, W. 2004, New Astronomy, submitted
- Yun, M. S., Ho, P. T. P., Lo, K. Y. 1994, Nature, 372, 530
- Zwaan, M. A. 2001, MNRAS 325, 1142